



Ultrafast cell-free DNA extraction from body fluids using UiO-66-NH₂ hydrogel packed syringe

Wang Pan^{a,1}, Dongyu Bao^{b,1}, Yaping Wang^c, Yifan Sun^d, Yue Jiang^a, Hui Yang^a, Shuo Liu^a, Guohua Zhou^{e,*}, Haiping Wu^{e,**}, Bin Wang^{a,c,***}

^a Clinical Stem Cell Center, Nanjing Drum Tower Hospital, Affiliated Hospital of Medical School, Nanjing University, Nanjing, 210008, China

^b Department of Stomatology, Nanjing Drum Tower Hospital, Affiliated Hospital of Medical School, Nanjing University, Nanjing, 210008, China

^c Clinical Stem Cell Center, Nanjing Drum Tower Hospital, Clinical Medical College of Traditional Chinese and Western Medicine, Nanjing University of Chinese Medicine, Nanjing, 210008, China

^d Department of Laboratory Medicine, Nanjing Drum Tower Hospital Clinical College of Jiangsu University, Nanjing, 210008, China

^e Department of Clinical Pharmacy, Jinling Hospital, State Key Laboratory of Analytical Chemistry for Life Science & Jiangsu Key Laboratory of Molecular Medicine, Medical School of Nanjing University, Nanjing, 210002, China

ARTICLE INFO

Keywords:

Liquid biopsy
Cell-free DNA
Metal-organic frameworks
Hydrogel
Solid-phase extraction
Syringe

ABSTRACT

Liquid biopsy represents a noninvasive or minimally invasive diagnostic approach relevant for both the organ-specific changes and systemic health conditions, whereas cell-free DNA (cfDNA) extraction from body liquids has attracted much attention in liquid biopsy, especially. Nowadays, metal-organic frameworks (MOF) such as UiO-66-NH₂ has been demonstrated efficient extraction property for DNA molecular, whereas the disadvantages of MOF for solid-phase extraction (SPE) still remain. Herein, one macro-pored MOF hydrogel formation strategy was constructed in this study to achieve superb extraction performance of cfDNAs from body fluids. The MOF crystals were embedded into sodium alginate, which was foamed using laurinol, pre-crosslinked through polyethyleneimine (PEI), and cured by zirconium ion at last. Validation of cfDNA extraction from human gingival crevicular fluid and plasma indicated that hydrogel beads allowed unimpeded flow of body fluids while enabling ultrafast extraction and elution of cfDNAs. Consequently, MOF hydrogel beads, when packed atop the syringe pintle as SPE column, achieved an efficient cfDNA extraction only within 6 min. Our construction strategy of extracting syringe provides an instrument-free purification modality of nucleic acid, which would tremendously simplify and quicken cfDNA extraction procedures for operators.

1. Introduction

Liquid biopsy (LB) involves the detection of targets from samples including any of body fluids *ex vivo*, including nucleic acids, proteins, and metabolites [1,2]. Meanwhile, LB represents a noninvasive or minimally invasive diagnostic approach relevant for both organ-specific changes and systemic health conditions [3]. In the last years, cell-free DNA (cfDNA) has garnered significant attention for diagnostic and treatment purposes, such as single nucleotide polymorphisms (SNPs) analysis and mutations detection [4]. SNPs are associated closely with susceptibility to various diseases, due to the proteins with different

alleles may exhibit variation in activities [5,6]. Conventionally, several hours are expended for finishing a genotyping interpretation from sample to result, including near 1 h for nucleic acid extraction, leading to delays in clinical medication guidance [7,8]. In emergency cases, patients need to be diagnosed or treated with drug as soon as possible, resulting notable clinical demand for method which could shrink time cost from nucleic acid extraction [9]. Moreover, the challenge of picking up very low abundance of one-base mutated cfDNA from body liquid remains, necessitating high standards for tumor-origin cfDNA extraction method [10].

Depending on the clinical challenge, an efficient and fast cfDNA

* Corresponding author.

** Corresponding author.

*** Corresponding author. Clinical Stem Cell Center, Nanjing Drum Tower Hospital, Clinical Medical College of Traditional Chinese and Western Medicine, Nanjing University of Chinese Medicine, Nanjing, 210008, China.

E-mail addresses: ghzhou@nju.edu.cn (G. Zhou), wuhaiping@smu.edu.cn (H. Wu), wangbin022800@126.com (B. Wang).

¹ Equal contribution to this study.

extraction method could achieve rapid SNP genotyping, thereby significantly reducing the detection time of LB. Nowadays, silica-based extraction columns have been mostly applied in solid-phase extraction (SPE) [11]. However, the combination between silica and nucleic acids typically requires high concentration of chaotropic salts, whereas their removal introduces alcohol reagents such as ethanol and isopropanol [12]. The dependence on organic reagents not only complicates the cfDNA extraction process, but also introduces additional impurities into elution products to affect downstream amplification. In this regard, the use of silica column is not conducive to efficient and rapid separation of cfDNA from body fluids, particularly point-of-care testing (POCT) [13]. Therefore, a material which can separate nucleic acid specially without the introduction of organic reagents from body fluids is highly desirable and meaningful.

In addition to the traditional materials, metal–organic frameworks (MOFs) are types of self-assembled synthetic materials with superb molecular separating ability from bulk solutions [14–16]. Recent research expounded an extraction method of cell-free nucleic acids using Ni-based MOF, whereas their release mechanism depending on MOF destruction through drastic pH changes [17,18]. In our previous work, one zirconium-based MOF named UiO-66-NH₂ has been demonstrated excellent water stability, together with superior DNA adsorption and desorption ability even under mild condition [19]. However, extraction column filled with primitive crystals is prone clogging due to the excessively small particle size of MOFs, resulting in failed DNA extraction from body fluids [20]. Fortunately, MOFs can be post-synthetic functionalized through various schemes, while their adsorption performance could retain. To this end, structuring MOFs into porous structure is considered an efficient mean.

Alginate is one of the most widely used biomaterials due to the simple hydrogel formatting method under mild conditions [21,22]. Additionally, the resulting beads offer embedding compatibility with almost any primitive materials, together with the properties maintaining of hydrogels and MOFs. In current, the performance of hydrogel beads containing MOFs was assessed in liquid separations under continuous flow [23,24]. However, collapse caused by freeze-drying and swelling during extraction could block the fluid across the beads, leading to a decrease in DNA adsorption efficiency. Therefore, a method for shaping novel MOF hydrogel to overcome these limitations is needed to enhance the utility of alginate beads in SPE of cfDNA from body fluids.

Herein, we describe a novel functionalized method for the preparation of composite beads consisting of UiO-66-NH₂ (referred to as U6N), sodium alginate (SA), polyethyleneimine (PEI), and zirconium ions. Firstly, U6N was well dispersed into the SA solution. Next, pre-crosslinking would be conducted to allow an unconsolidated structure before the formation of hydrogel beads, with an appropriated amount of PEI added [24]. Immediately after, the hydrogel system was vortexed with oil phase for micro-spherization. Importantly, laurinol was used as oil phase during vortex instead of mineral oil in order to introduce more macropores within the hydrogel beads. Finally, the emulsion was poured into the zirconium curing solution and then stirred rapidly. The resulting porous hydrogel beads contained an abundance of U6N crystals, together with suitable swelling and mechanical properties. Moreover, the hydrogel beads avoided the blockage during nucleic acid extraction effectively, while the extraction process is simplified tremendously. Consequently, the multifaceted properties of the hydrogel beads reveal their superb performance as column fillers for nucleic acid extraction. Furthermore, the porous U6N beads were utilized for ultrafast cfDNA extraction using syringes from gingival crevicular fluid (GCF) and plasma in our study, indicating their application potential in point-of-care testing (POCT).

2. Experimental section

2.1. Chemicals and materials

2-Aminoterephthalic acid (NH₂-H₂BDC) was purchased from Shanghai Maclin Biochemical Co., Ltd. (Shanghai, China). Ethanol, acetic acid, and Tween-20 were supplied by Nanjing Chemical Reagent Co., Ltd. (China). Zirconium chloride (ZrCl₄), sodium alginates (SA), sodium hydroxide (NaOH), sodium chloride (NaCl), Potassium chloride (KCl), N, N-dimethylformamide (DMF), disodium hydrogen phosphate (Na₂HPO₄), and potassium dihydrogen phosphate (KH₂PO₄) were supplied by Sinopharm Chemical Reagent Co., Ltd. (China). RIPA lysis buffer was from Beijing Solarbio Science & Technology Co., Ltd. Laurinol and mineral oil was purchased from Chinasun Specialty Products Co., Ltd. (China). The nucleic acid extraction kit was from Qiagen (52904, Germany). All the reagents were used as received.

SYBR Green Mix (TC015) and TaqMan Mix (TC009) was from Starbio (Suzhou, China). All oligonucleotides were synthesized from GenScript Biotech Corporation (Nanjing, China).

Clinical samples were collected from donors with signed informed consent forms at Jinling Hospital (Nanjing, China) and Drum Tower Hospital (Nanjing, China).

2.2. Measurement and apparatus

The crystallinity of the obtained products was determined by X-ray Diffraction (XRD, Thermo Fisher Scientific X'TRA). The Surface morphology and Energy Dispersive Spectrometer (EDS) analyses were performed by Scanning Electron Microscopy (SEM, Zeiss, Ultra Plus). The morphology and microstructural analyses were performed by TEM (JEOL-2010). Fourier Transform Infrared Spectroscopy (FT-IR) analyses were performed by a Nicolet iS10 FI-IR spectrometer. N₂ adsorption-desorption investigation and pore size distribution were performed by ASAP2460 (Micromeritics, USA).

2.3. Synthesis of UiO-66-NH₂

UiO-66-NH₂ was synthesized based on a typical solvothermal protocol modified slightly by changing the amount of acetic acid [19]. 2-aminoterephthalic acid (0.45 mmol) and ZrCl₄ (0.45 mmol) were dissolved in 30 mL of DMF, together with 72 mmol of acetic acid inside. The solution was then transferred into a Teflon-lined autoclave, followed by heating at 120 °C for 24 h. After cooling to room temperature, the prepared product was washed three times with DMF and then dispersed in methanol for 3 days to remove the residual DMF molecules. Finally, the obtained product was washed with ethanol and then dried thoroughly under vacuum at 90 °C.

2.4. Formation of UAZPF

Firstly, 15 mg of sodium alginate was dissolved in 1 mL of ddH₂O, followed by dispersing 75 mg of U6N in the solution through ultrasonic. Next, 5 µL of PEI was dissolved in 0.5 mL of ddH₂O, while 3 mL of foaming agent (laurinol: methanol = 9:1) was prepared at the same time. Meanwhile, the curing solution was prepared by dissolving 395 mg of ZrCl₄ in 30 mL of ddH₂O. Afterwards, PEI solution and foaming agent was added into SA-U6N suspension in order, followed by beads formatting through vortex violently. Immediately after, the system was poured into the pre-heated curing solution accompanied by stirring fast. The hydrogel products were then washed by 70 % ethanol for several times after fully cured. Finally, the UAZPF beads were obtained after a freeze-drying step.

As a contrast, 3 mL of mineral oil was used instead of foaming agent during beads formatting to obtain UAZP hydrogel, while the AZP hydrogel is prepared by SA solution instead of SA-U6N suspension comparing with UAZP.

2.5. qPCR reaction

Each 20 μ L of fluorescent qPCR mixture of the experiment group contained 10 μ L of SYBR Green Mix, 0.5 μ M of each PCR primer, 2 μ L of extraction products, and the remainder of water. The negative control group contained 10 μ L of SYBR Green Mix, 0.5 μ M of each PCR primer, and the remainder of water. The qPCR program was 95 $^{\circ}$ C for 3 min, followed by the amplification of targets for 45 cycles at 95 $^{\circ}$ C for 10 s, 60 $^{\circ}$ C for 15 s, and 72 $^{\circ}$ C for 20 s. The signal was obtained after each cycle using a QuantStudio™ 6 Flex.

Each 20 μ L of TaqMan qPCR mixture of the experiment group contained 10 μ L of TaqMan Mix, 0.5 μ L of each PCR primer, 0.5 μ L of FAM and VIC probes respectively, 2 μ L of extraction products, and the remainder of water. After pre-degeneration under 95 $^{\circ}$ C for 3 min, the amplification of VDR-Fok I was performed for 40 cycles at 95 $^{\circ}$ C for 10 s, 61.5 $^{\circ}$ C for 15 s, and 72 $^{\circ}$ C for 20 s, the amplification of CYP2C9*3 was performed for 50 cycles of 95 $^{\circ}$ C for 10 s, 57 $^{\circ}$ C for 15 s, and 70 $^{\circ}$ C for 20 s. Similar but different, each 20 μ L of ARMS-PCR mixture of the experiment group contained 0.5 μ L of FAM probes only, while the other compositions were corresponded as above. After pre-degeneration, the amplification of L858R was performed for 50 cycles of 95 $^{\circ}$ C for 10 s, 54 $^{\circ}$ C for 15 s, and 65 $^{\circ}$ C for 20 s. The signal was obtained after each cycle using a QuantStudio™ 6 Flex as well.

The specific primer and probe for targets were designed according to Table 1.

2.6. DNA extraction procedure

In the extraction procedure in tube, 2 mg of UiO-66-NH₂ or hydrogel beads was added to a 1.5 mL centrifuge tube containing 0.2 mL of ATP-5B DNA template solution with 10⁶ copies inside. The system was then incubated for 10 min under gentle oscillation. In sequence, the MOFs/hydrogel beads were centrifuged for 1 min at 4000 \times g, and the precipitate was resuspended in 0.9 % NaCl solution to remove residual impurities. After the washing step, the hydrogels were centrifuged again for 1 min at 4000 \times g, and the supernatant was discarded. Then, 0.1 mL of 10 mM phosphate-buffered saline (PBS) was added, and the tube was incubated for 5 min to elute the DNA templates.

In the extraction procedure using syringes, a syringe extractor was firstly installed as follow: 1) a piece of cotton was filled in the bolt of needle; 2) about 2 mg of hydrogel beads was packed onto the cotton as extraction column; 3) a piece of cotton was put on the column; 4) the whole needle was installed on the syringe at the end. Next, four 1.5 mL centrifuge tubes containing different solutions were arranged as follow: 1) 0.5 mL of 0.9 % NaCl solution; 2) 0.2 mL sample; 3) 0.6 mL of 0.9 % NaCl solution; 4) 30 μ L of PBS (10 mM). Finally, the extraction steps were operated as follow: 1) saline in tube 1 was aspirated into the syringe to madefact the column; 2) sample in tube 2 was aspirated into the syringe, and the solution in the syringe was pushed out slowly

afterwards; 3) saline in tube 3 was aspirated into the syringe and pushed out fast, whereafter the column was blown several times; 4) PBS in tube 4 was aspirated to soak the column for 1 min, and the elution product was dropped into the tube at the end.

The cycle threshold (Ct) value is the number of cycles when the fluorescent signal in each reaction tube reaches the set threshold. The DNA recovery rate was verified by comparing the Δ Ct values between the experimental and positive control groups. The specific formula was derived as follows:

$$X_{Ct} = X \times 2^{Ct}$$

$$\lg X_{Ct} - \lg X = Ct \times \lg 2$$

$$Ct = (\lg X_{Ct} - \lg X) / \lg 2$$

$$\Delta Ct = Ct_2 - Ct_1$$

$$\Delta Ct = (\lg X_{Ct} - \lg X_2) / \lg 2 - (\lg X_{Ct} - \lg X_1) / \lg 2$$

$$\Delta Ct = (\lg X_1 - \lg X_2) / \lg 2$$

$$\Delta Ct = -\lg (X_2 / X_1) / \lg 2$$

$$\text{Recovery rate} = X_2 / X_1 \times 100\%$$

$$\text{Recovery rate} = 2^{-\Delta Ct} \times 100\%$$

Herein, X_{Ct} represents the amount of DNA amplicons at the PCR cycle Ct. Ct_1 represents the number of cycles when the fluorescent signal of the positive control reaches the threshold at the input DNA template amount of X_1 . Ct_2 is the number of cycles in each test group at the DNA target amount of X_2 (the amount of DNA after extraction).

2.7. Molecular dynamics simulation

The adsorption mechanism and conformation between oligonucleotide and MOF was performed by MOE 2020. CIF data of UiO-66-NH₂ was obtained from Cambridge Crystallographic Data Centre (CCDC), and then packed as surface of U6N surface. The parameters were carried out in Amber10: EHT forcefield, while the hydrogens, lone pairs were adjusted, and partial charges were calculated. 1000 ps MD simulation was performed in a water environment with pH 7.0, the U6N position was restrained, while oligonucleotide was free to move. Simulations were carried out with a time step of 0.5 ps and data were saved each step.

2.8. Statistical analysis

At least three replicates of each data were listed as the mean \pm standard derivation (SD) of for each experiment. Then data were

Table 1
Sequences of the primers and probes utilized for qPCR.

#	Name	Primer	Probe
1	ATP-5B	Forward: CAGCAGATTITGGCAGGTGAATA Reverse: GACAAAGACCCCTCACGAT	
2	ACTB-1	Forward: GGCCTCTGGCCGTACCACTG Reverse: GCCAGGTCCAGACGCAGGAT	
3	ACTB-2	Forward: CCAAGGCCAACCCGCGAGAAG Reverse: GTACGGCCAGAGGCGTACAGG	
4	ACTB-3	Forward: CCCCTGAACCCCAAGGCCAA Reverse: GGTACGGCCAGAGGCGTACAG	
5	VDR-Fok I	Forward: TGGCCTGCTTGTCTGT Reverse: CTCGGTCTCCACACA	FAM: CTTACAGGGATGGAGGCAATG VIC: CTTACAGGGACGGAGGCAATG
6	CYP2C9*3	Forward: TGTGGTGACACGAGGT Reverse: CCTTGGGAATGAGATAG	FAM: AGAGATACATTGACCTTCTCC VIC: AGAGATACCTTGACCTTCTCC
7	EGFR-L858R	Forward: ACAGATTTTGGGCG Reverse: AGCCACCTCCTTAC	FAM: CCAAACCTGCTGGGTGC

presented and analyzed by unpaired parametric test with Welch's correction through the software GraphPad Prism (8.0.2, GraphPad Software, USA), and a $p < 0.05$ was considered statistically significant.

3. Results and discussion

3.1. Formation and characterization of UAZPF

UiO-66-NH₂ (hereinafter referred to as U6N) particles were prepared by solvothermal method. UAZPF represents U6N particles embedded in

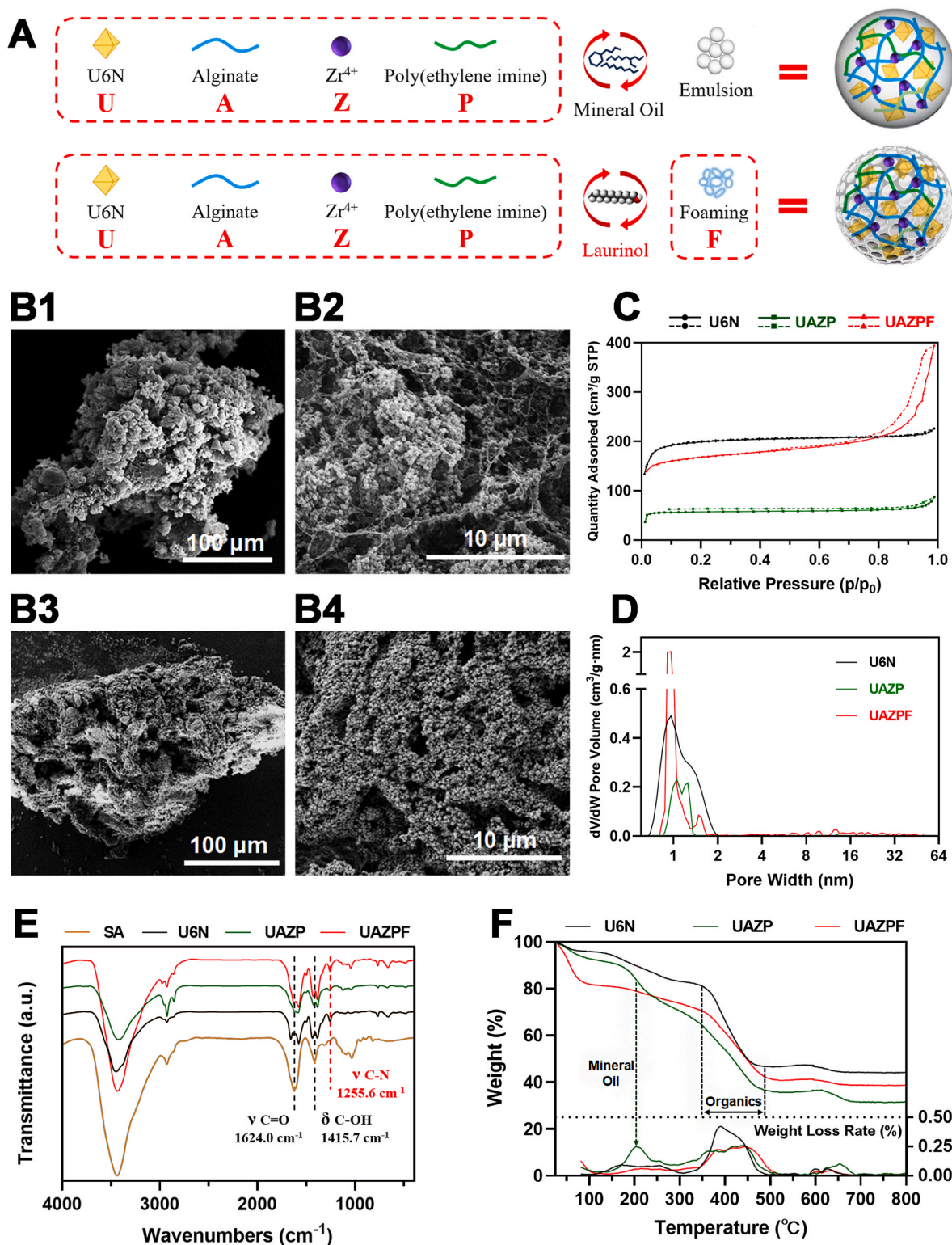
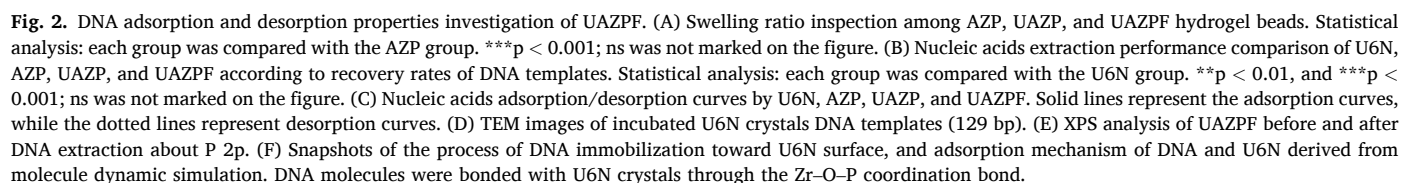


Fig. 1. Schematic diagram and characterizations. (A) Formation scheme of UAZP and UAZPF hydrogel beads. (B) SEM images of UAZP and UAZPF at different magnification. (C–F) Characterizations of U6N, UAZP, and UAZPF about (C) N₂ adsorption-desorption isotherms, (D) pore size distributions, (E) FT-IR spectrums, and (F) TGA curves and weight loss curves.

macropores were constructed due to the tiny bubbles introduced by laurinol among the UAZPF hydrogel beads without negative affection of U6N embedding (Fig. 1B). Additionally, SEM characterization of AZP hydrogel revealed a typical porous structure, which was maintained well in UAZP and UAZPF during formatting (Fig. S1). Nitrogen physisorption isotherms showed a hysteresis loop around relative pressure 0.8 to 1.0 in UAZPF group, indicated more macropores of UAZPF than UAZP and



primitive U6N crystals (Fig. 1C). Otherwise, the micropore distribution of UAZPF maintained well, while the extra pores introduced by laurinol even increased the micropore volume (Fig. 1D). The calculated Brunauer–Emmett–Teller (BET) surface area of the three materials was 803.5988 m²/g (U6N), 261.6878 m²/g (UAZP), and 646.9726 m²/g (UAZPF), whereas the pore volume was 0.350004 cm³/g, 0.135307 cm³/g, and 0.610522 cm³/g, correspondingly (Table S1). The well BET surface area retaining and the best pore volume performance of UAZPF indicated better fluid permeability of UAZPF and superior potential of UAZPF for nucleic acid adsorption. Moreover, XRD showed the crystallinity and integrity of U6N crystals were retained well in both UAZP and UAZPF hydrogel beads (Fig. S2). FT-IR indicated that UAZP and UAZPF maintained the stretching vibration of C–N from aromatic amine in U6N crystals at 1255.6 cm⁻¹, while the characteristic peaks of carboxylate from UAZP and UAZPF, such as in-plane bending vibration at 1415.7 cm⁻¹ and stretching vibration at 1624.0 cm⁻¹, showed cleavage peaks similar to that of U6N (Fig. 1E). Additionally, thermogravimetric analysis showed similar curves among U6N, UAZP and UAZPF, which indicated the predominance of U6N in both hydrogel beads. Further analysis demonstrated the weight loss rates between 350 °C and 488 °C were relatively high in all groups due to the organics loss among them. Differently, the weight loss rate around 202 °C in UAZP was much higher than other groups, which could be attributed to the residue of mineral oil during hydrogel formation (Fig. 1F). Moreover, UAZPF hydrogel beads showed no significant collapse after soaking in both normal saline and lysis buffer for 5 days, which demonstrated the superb stability of this formation method (Fig. S3).

Preliminary summary, UAZPF hydrogel beads were constructed through vortex using U6N-SA-PEI mixture and laurinol foaming agent, followed by curing with ZrCl₄ solution. Although UAZP and UAZPF hydrogel beads both showed micrometer to millimeter scale with porous structure inside, the additional pores caused by foaming agent allowed UAZPF better property utilization of alginate hydrogel than UAZP, which indicated superior potential for column packing in extraction. Besides, laurinol is much easier to remove than mineral oil after hydrogel beads curing, simply by lowering the temperature of solution below 23 °C.

3.2. Investigation of DNA extraction performance

The swelling ratio AZP, UAZP, and UAZPF was 223.22 %, 264.30 %, and 928.83 %, respectively (Fig. 2A). UAZPF showed significantly higher swelling property than other groups because of the macropores within UAZPF, resulting in superior target molecules extraction potential from solution. Next, quantified PCR amplification products of ATP-5B (129 bp) were utilized to further investigate the extraction performance of each group. The DNA recovery rate was calculated using the formula converted from the ΔCt value. DNA templates were extracted efficiently by each group except AZP, with recovery rates of 75.23, 9.53, 72.80, and 84.80 %, respectively (Fig. 2B). Next, the adsorption and desorption performance of each group was investigated by mixing hydrogel beads with DNA templates and PBS (10 mM) in sequence. The concentration of DNA templates decreased rapidly within 1 min in UAZPF group, whereas the UAZP group showed slightly inferior performance (Fig. 2C). Moreover, the U6N group showed slower extraction rate and lower adsorption percentage than UAZPF group, while the adsorption performance of AZP group was the worst. Correspondingly, most of the DNA templates were eluted within 1min from UAZPF, whereas the other groups showed relatively poor performance. In brief, DNA molecules could be extracted and eluted rapidly and thoroughly from UAZPF compared with other groups. The superb adsorption and desorption ability of UAZPF hydrogel beads could be attributed to the common effects with porous structure, high U6N content, and additional zirconium incorporation. Additionally, the DNA recovery rate of 5 UAZPF batches showed no significant difference with each other, indicated the reproducibility of this hydrogel formation method (Fig. S4).

As shown in Fig. 2D, TEM result indicated that DNA molecules could be adsorbed on the U6N surface densely. Correspondingly, X-ray photoelectron spectroscopy demonstrated the emergence of phosphorus characteristic peak after extraction by UAN crystals to DNA molecules (Fig. 2E). Molecular dynamics (MD) simulations were performed to clarify the binding conformation between DNA and U6N nanoparticles. The simulation suggested that the double-stranded DNA molecule was partially bond on the U6N surface, with DNA-MOF binding being quick and stable. Further analysis clarified the bonding mechanism. As shown in Fig. 2F, Zr–O–P coordination bond was observed after MD simulation. Notably, Zr–O–P coordination bonds require more investigation because of the direct interaction between Zr and O clusters and the phosphate skeleton, while this coordination bond has been found important for DNA adsorption. These findings indicated the appropriate properties of UAZPF in nucleic extraction, which also suggested the point-of-care testing (POCT) potential of this novel hydrogel in nucleic acid extraction because of its extremely fast and efficient DNA recovery performance.

3.3. Construction and investigation of UAZPF syringe

Based on the superb nucleic acid binding property, the potential of UAZPF for POCT was investigated further. Therefore, a simple syringe device was designed as shown in Fig. 3A, which could be assembled ultrafast. The syringe was engineered to operate using only basic laboratory equipment with a time cost within 6 min following the operation schematic diagram (Fig. 3B). After DNA recovery using UAZPF syringe, the recovery rate of ATP-5B DNA templates diluted with lysis buffer was 18.17 %, and the recovery rate was 77.50 % while the lysis buffer was replaced with normal saline (Fig. 3C). The significant difference between these two groups could be attributed to the creation of massive bubbles of liquid phase during the extraction operations, especially passing through the extraction column. The bubbles would block the adsorption sides of UAZPF, resulting in a decrease of extraction performance of the hydrogel. Therefore, the UAZPF syringe device was expected to directly extract nucleic acids in fluids to enrich trace number of nucleic acids for downstream analysis. The cell-free DNAs (cfDNAs) in the supernatant of cultured cells were extracted by UAZPF syringe or commercial kit, followed by verification using three pairs of primers targeting the ACTB gene (Fig. 3D). The amplification curves were similar whether using UAZPF syringe or commercial kit, indicating the efficient cfDNA extraction performance of UAZPF hydrogel beads, together with the ultrafast and convenient extraction operation (Supplement Video). Besides, the recovery rate of UAZPF syringe showed a significant decreased since the second cycle of DNA extraction, which could attribute to the phosphate sealing after DNA elution (Fig. S5). Therefore, we aimed to apply UAZPF syringe into cfDNA extraction from body liquids, which could further delineate the potential of this device in point-of-care testing (POCT).

3.4. Evaluation with gingival crevicular fluid samples

Gingival crevicular fluid (GCF) is referred to the fluid that penetrates from the gum connective tissue into the gingival sulcus through the intrasulcus epithelium and the conjunctive epithelium, which contains various components derived from serum, adjacent periodontal tissues, and bacteria [25]. GCF is obtained in a very simple and non-invasive manner (Fig. S6), which is considered an ideal liquid biopsy sample since wealth of information about human body could be reflected. Therefore, the cfDNAs contained in GCF are available to provide information through ultrafast purification using the UAZPF syringe. Recently, the single nucleotide polymorphism (SNP) of VDR-Fok I (rs2228570) has been reported relevant to periodontitis, for the conformation change of VDR receptor affects the viability of osteoclasts in alveolar bone [26]. The principle of using TaqMan probe method to detect SNP of VDR-Fok I locus in eluted products is shown in Fig. 4A. As

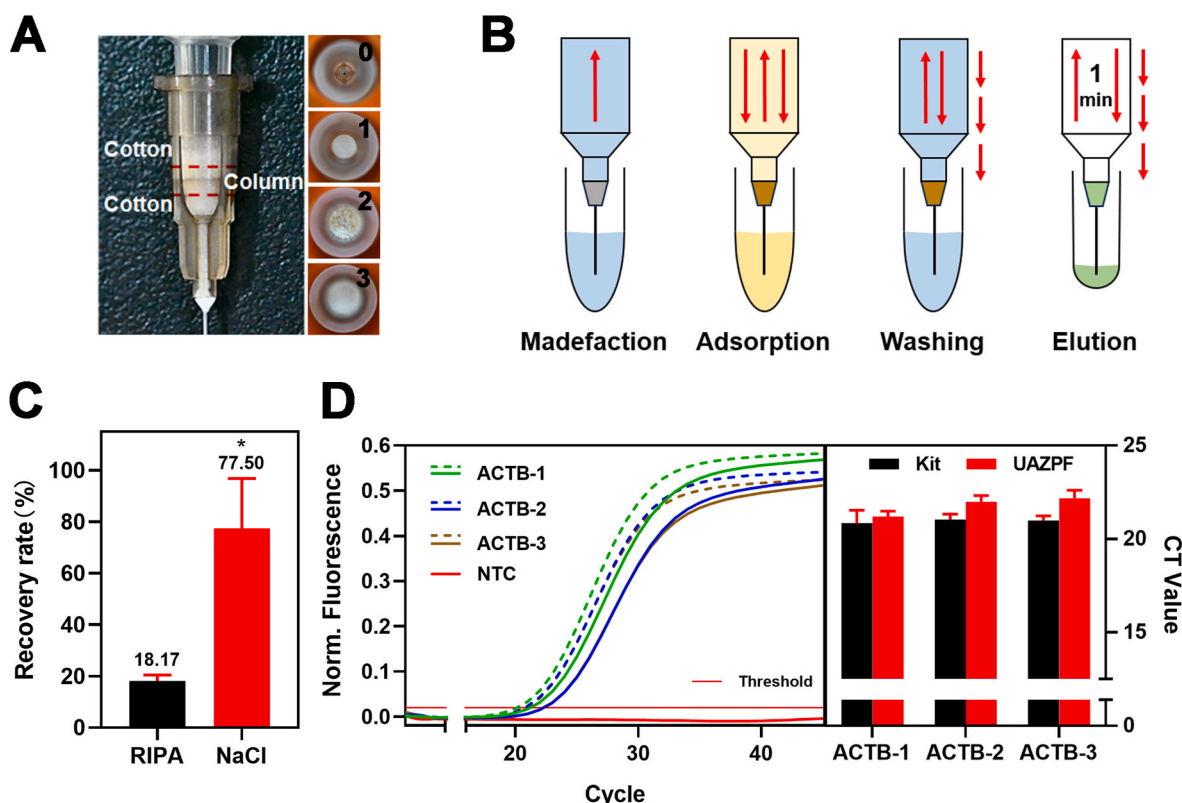


Fig. 3. Assembly and investigation of UAZPF syringe. (A–B) Schematic representation of (A) UAZPF syringe device assembly, and (B) DNA extraction using UAZPF syringe. (C) DNA recovery rate inspection of UAZPF syringe toward DNA templates dissolved in RIPA lysis buffer or normal saline, respectively. (D) Comparison of cfDNA extraction performance between UAZPF syringe and commercial kit. Solid lines represent the amplification curves of the DNA products extracted by UAZPF, and the dotted lines represent those of the commercial kit. Statistical analysis: * $p < 0.05$; ns was not marked on the figure.

comparisons, cfDNA purified by commercial extraction kit showed sample amplification results to those of UAZPF syringe, whereas GCF from volunteer could hard to be amplified directly because of very low abundance of targets with impurities interference (Fig. 4B). 9 amplification curves of extraction products from volunteers showed the same results between UAZPF syringe and commercial kits, regardless of whether the SNP genotyping was FF, Ff, or ff. Another 9 amplification results also demonstrated the comparable performance between UAZPF syringe and commercial kit (Fig. S7). These results indicated that the UZAPF syringe could absolutely satisfy the demand of trace cfDNA extraction in GCF, resulting in significant extraction operations simplification and substantial reduction in extraction duration.

3.5. Evaluation with plasma samples

Plasma from patients hold much information of interest and is already one of the most used body fluids in liquid biopsy [2]. However, trace amounts of cfDNAs are overwhelmed by various impurities in plasma, resulting in higher risk of extraction column clogging compared with other body liquids. Fortunately, the macro-porous structures within UAZPF hydrogels would not only facilitate the liquid flowing inside the beads, but also offset the risk extraction column plugging caused by hydrogel swelling and impurities from samples. CYP2C9 is one of the drug metabolizing enzymes that could reflect the metabolic rate and efficacy of drugs such as warfarin, with multiple SNP genotyping. As shown in Fig. 5A, the amplification results of clinical plasma samples purified by UAZPF syringe from patients undergoing heart valve replacement demonstrated the exact same SNP genotyping of CYP2C9*3 compared to pyrosequencing interpretations, correspondingly. The amplification curves of products extracted from other 15 plasma were same to known genotypes one to one correspondence (Fig. S8).

Besides, the UAZPF syringe could also be applied in circulating tumor DNA (ctDNA) extraction for convenient mutation detection of patients, while the operation and cost would able to be reduced tremendously. For instance, some mutant-targeted medicines such as gefitinib and erlotinib are much more effective than traditional chemotherapy drugs in non-small cell lung cancer (NSCLC) treatment if the EGFR gene of a patient has L858R mutation [27]. As shown in Figs. 5B and 4 plasma samples in 11 patients showed L858R mutation using ARMS-PCR, whether after UAZPF syringe extraction or commercial kit purification, while the amplification curves of the remaining 7 elution products showed negative results, correspondingly (Fig. S9). In most cases, the blood samples of patients were only detected for traditional cancer biomarkers associated with lung cancer, while pathology reports also indicated only positive/negative classification among several markers. However, real-time monitoring of cancer biomarkers plays an important role in precise treatment of the patient [27]. Benefit of the UAZPF syringe, one-base mutated ctDNA at a very low abundance could be picked up specifically from blood with tremendous fast and convenient operation. Moreover, the relatively low cost of the syringe device compared with commercial kit offered patients higher acceptance about genetic testing.

Looking forward to further, the UAZPF syringe showed superb potential of providing high-quality nucleic acid templates for instrument-free detection, together with shrinking the time cost of genetic testing conspicuously. Meanwhile, the UAZPF hydrogel beads indicated possibility of being compatible with extraction chip to achieve the prospect of “sample-in-answer-out”.

4. Conclusion

In Summary, UiO-66-NH₂ (U6N) was embedded into macro-pored

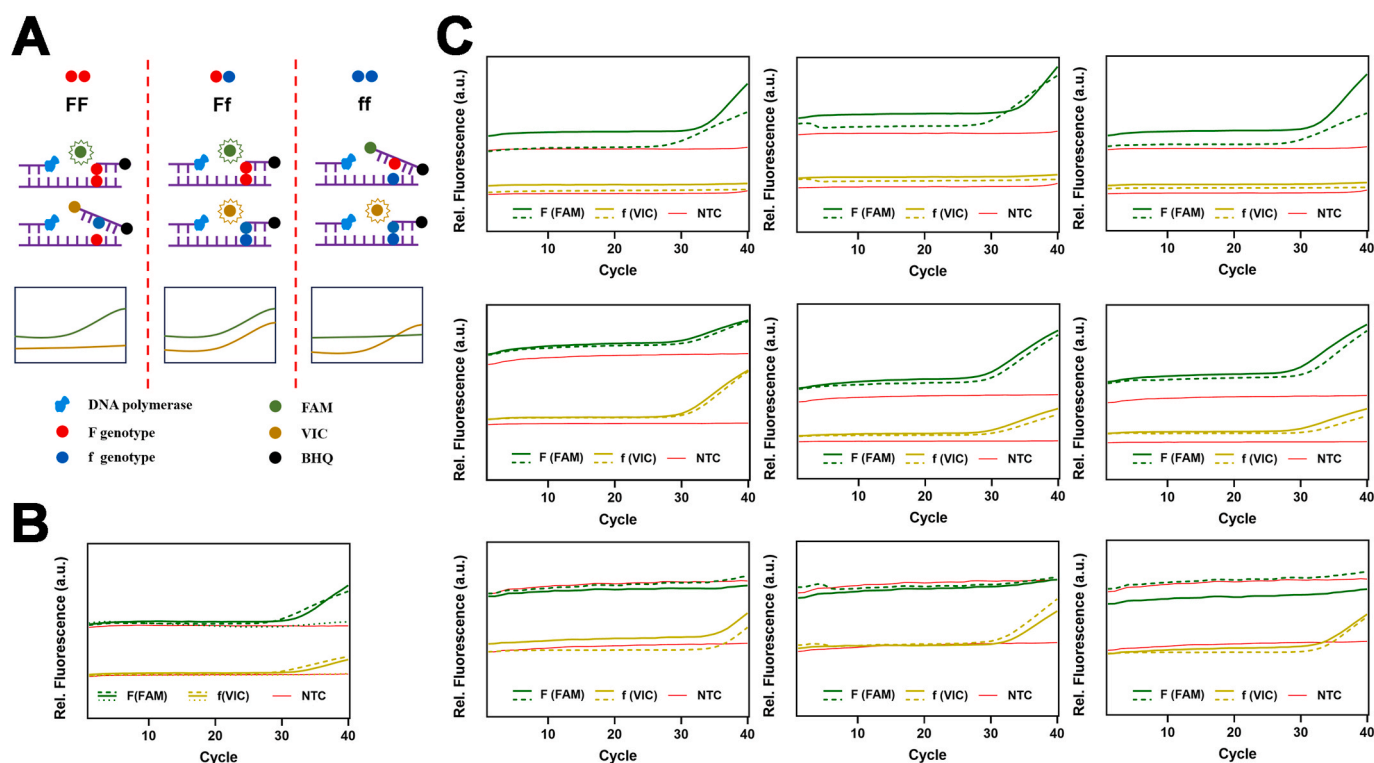


Fig. 4. Comparison of cfDNA extraction results from gingival crevicular fluid between UAZPF syringe and commercial kit. (A) Schematic representation of SNP determination by TaqMan probe technique. (B–C) Comparison of the cfDNA extraction performance from GCF of volunteers between UAZPF syringe and commercial kit. Short-dotted lines represent amplification curves using GCF samples directly (B), solid lines represent the amplification curves of the DNA products extracted by UAZPF, and long-dotted lines represent those of the commercial kit.

hydrogel beads named UAZPF in order to achieve better extracting efficiency of cfDNAs from body fluids than other schemes. U6N has specific adsorption ability of nucleic acids due to Zr–O–P coordination, while solution with appropriate phosphate concentration would elute nucleic acids competitively. Moreover, the extracting operation eliminated the dependence on chaotropic salts and alcohols, which make the process simpler and faster than traditional methods. Importantly, our novel hydrogel formation protocol maintained the nucleic acids adsorption and desorption abilities well, even the U6N crystals were encapsulated inside. This property of UAZPF could be attributed not only to the porous structure formation during the pre-crosslinking between sodium alginate (SA) and polyethyleneimine (PEI), but also the solidification of SA-based hydrogel through $ZrCl_4$. Furthermore, extra macropores were introduced inside the beads due to the laurinol frothier during vortex. Under the function of these factors, UAZPF hydrogel beads allowed body fluids flowing unimpeded, while the contained cfDNAs were adsorbed ultrafast, together with a tremendous simplification of washing and elution operations. Therefore, UAZPF hydrogel beads were packed on the syringe pintle as column for solid-phase extraction (SPE), which have achieved fast and instrument-free cfDNA extraction within 6 min from body fluids. The purification products from both gingival crevicular fluid (GCF) and plasma extracted by UAZPF syringe satisfied the need of downstream amplification. The construction strategy of UAZPF syringe provides potential to be compatible with more convenient detection method to prospect for point-of-care testing (POCT).

CRediT authorship contribution statement

Wang Pan: Writing – review & editing, Writing – original draft, Visualization, Validation, Supervision, Software, Resources, Project administration, Methodology, Investigation, Formal analysis, Data curation, Conceptualization. **Dongyu Bao:** Writing – original draft,

Supervision, Resources, Project administration, Methodology, Investigation, Data curation. **Yaping Wang:** Validation, Software, Project administration, Methodology, Investigation, Data curation. **Yifan Sun:** Visualization, Validation, Software, Methodology. **Yue Jiang:** Software, Formal analysis, Data curation. **Hui Yang:** Resources, Funding acquisition. **Shuo Liu:** Validation, Funding acquisition. **Guohua Zhou:** Writing – review & editing, Writing – original draft, Validation, Resources, Formal analysis, Conceptualization. **Haiping Wu:** Writing – review & editing, Writing – original draft, Resources, Project administration, Methodology, Formal analysis, Conceptualization. **Bin Wang:** Writing – review & editing, Writing – original draft, Validation, Supervision, Resources, Project administration, Methodology, Investigation, Funding acquisition, Formal analysis, Data curation, Conceptualization.

Fundings

This study was supported by National Natural Science Foundation of China (NSFC 81571213 and 82070459), Key Project of Jiangsu Province (BE2020765), Project of Modern Hospital Management and Development Institute, Nanjing University/Aid project of Nanjing Drum Tower Hospital Health, Education & Research Foundation (NDYG2020030), and Jiangsu Biobank of Clinical Resources (BM2015004, Bin Wang). Additionally, Natural Science Foundation of Jiangsu Province (BK20230141, Hui Yang) and Nanjing Medical Science and Technique Development Foundation (YKK23089, Shuo Liu) also supported this study.

Declaration of competing interest

The authors declare that they have no known competing financial interests or personal relationships that could have appeared to influence the work reported in this paper.

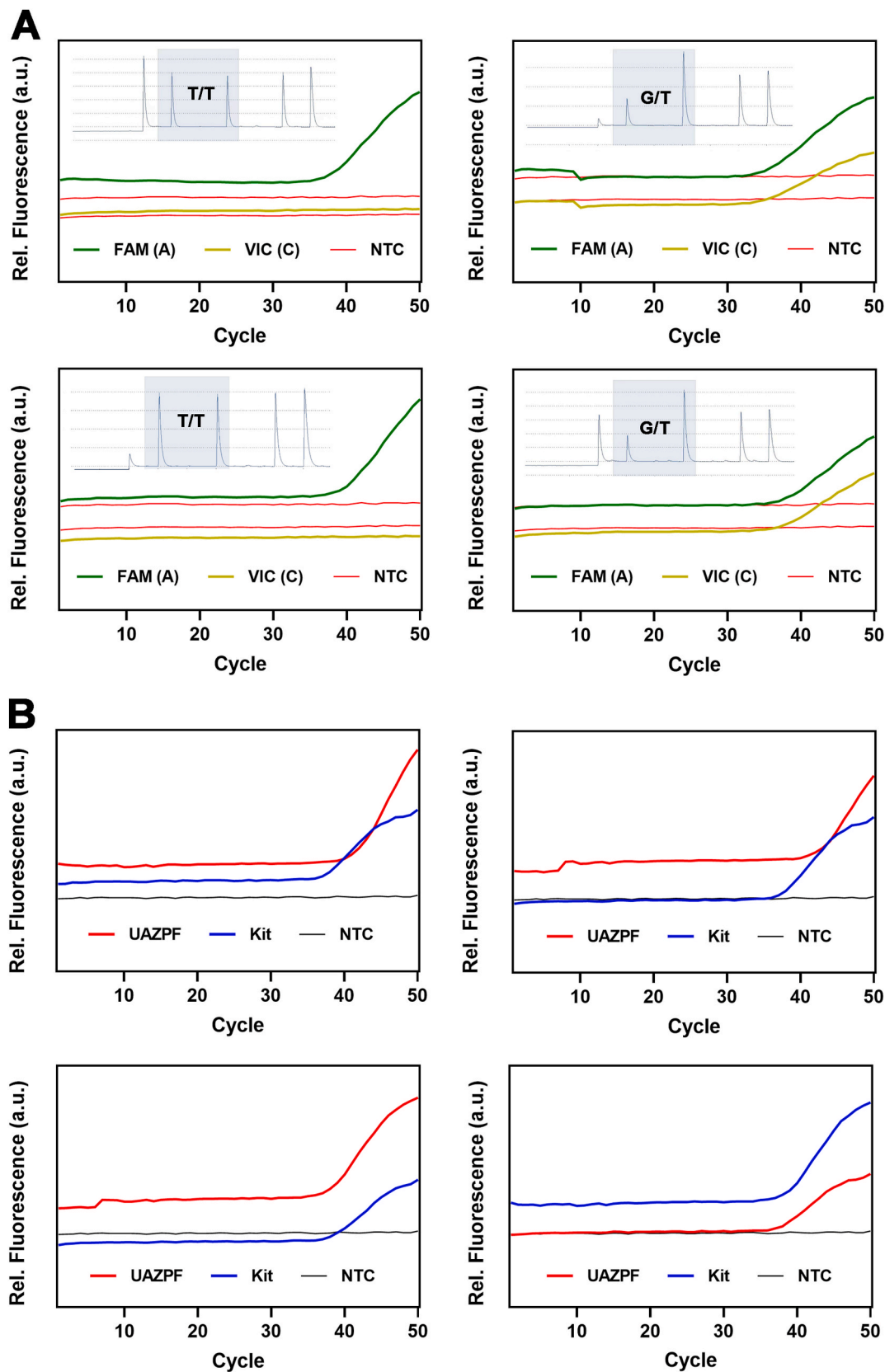


Fig. 5. Comparison of cfDNA extraction results from plasma between UAZPF syringe and commercial kit. (A) Comparisons of cfDNA extraction performance by UAZPF syringe to pyrosequencing interpretations. (B) Comparison of the ctDNA extraction performance from plasma of lung cancer patients between UAZPF syringe and commercial kit.

Appendix A. Supplementary data

Supplementary data to this article can be found online at <https://doi.org/10.1016/j.talanta.2025.127867>.

Data availability

Data will be made available on request.

References

- [1] L. Gorgannezhad, M. Umer, M.N. Islam, N.T. Nguyen, M.J.A. Shiddiky, Circulating tumor DNA and liquid biopsy: opportunities, challenges, and recent advances in detection technologies, *Lab Chip* 18 (8) (2018) 1174–1196, <https://doi.org/10.1039/C8LC00100F>.
- [2] B. Michela, Liquid biopsy: a family of possible diagnostic tools, *Diagnostics* 11 (8) (2021), <https://doi.org/10.3390/diagnostics11081391>.
- [3] C. Gerner, V. Costigliola, O. Golubnitschaja, Multiomic patterns in body fluids: technological challenge with a great potential to implement the advanced paradigm of 3p medicine, *Mass Spectrom. Rev.* 39 (5–6) (2020) 442–451, <https://doi.org/10.1002/mas.21612>.
- [4] K. Martin, P. Dar, C. MacPherson, M. Egbert, Z. Demko, S. Parmar, K. Hashimoto, S. Haeri, F. Malone, R.J. Wapner, A.S. Roman, A. Khalil, R. Faro, R. Madankumar, N. Strong, R.M. Silver, N. Vohra, J. Hyett, M. Rabinowitz, C. Kao, H. Hakonarson, B. Jacobsson, M.E. Norton, Performance of prenatal cfDNA screening for sex chromosomes, *Genet. Med.* 25 (8) (2023) 100879, <https://doi.org/10.1016/j.gim.2023.100879>.
- [5] S.L. Morais, J. Magalhaes, V.F. Domingues, C. Delerue-Matos, J. Ramos-Jesus, H. Ferreira-Fernandes, G.R. Pinto, M. Santos, M.F. Barroso, Development of an electrochemical DNA-based biosensor for the detection of the cardiovascular pharmacogenetic-altering SNP CYP2C9*3, *Talanta* 264 (2023) 124692, <https://doi.org/10.1016/j.talanta.2023.124692>.
- [6] C. Zhai, Y. Zhao, Z. Zhang, X. Wang, L. Li, J. Li, Mechanism of multifunctional adaptor protein SHARPIN regulating myocardial fibrosis and how SNP mutation affect the prognosis of myocardial infarction, *Biochim. Biophys. Acta, Mol. Basis Dis.* 1870 (8) (2024) 167467, <https://doi.org/10.1016/j.bbdis.2024.167467>.
- [7] L. Zhang, X. Ma, D. Liu, J. Shan, Y. Chu, J. Zhang, X. Qi, X. Huang, B. Zou, G. Zhou, Visualized genotyping from "sample to results" within 25 minutes by coupling recombinase polymerase amplification (RPA) with allele-specific invasive reaction assisted gold nanoparticle probes assembling, *J. Biomed. Nanotechnol.* 18 (2) (2022) 394–404, <https://doi.org/10.1166/jbn.2022.3258>.
- [8] M. Zhang, Y. Liu, L. Chen, S. Quan, S. Jiang, D. Zhang, L. Yang, One simple DNA extraction device and its combination with modified visual loop-mediated isothermal amplification for rapid on-field detection of genetically modified organisms, *Anal. Chem.* 85 (1) (2013) 75–82, <https://doi.org/10.1021/ac301640p>.
- [9] J. Stam, Thrombosis of the cerebral veins and sinuses, *N. Engl. J. Med.* 352 (17) (2005) 1791–1798, <https://doi.org/10.1056/NEJMra042354>.
- [10] F. Yu, K.W. Leong, G.M. Makrigiorgos, Nuclease-assisted, multiplexed minor-allele enrichment: application in liquid biopsy of cancer, *Methods Mol. Biol.* 2394 (2022) 433–451, https://doi.org/10.1007/978-1-0716-1811-0_22.
- [11] P. Guha, A. Das, S. Dutta, T.K. Chaudhuri, A rapid and efficient DNA extraction protocol from fresh and frozen human blood samples, *J. Clin. Lab. Anal.* 32 (1) (2018), <https://doi.org/10.1002/jcla.22181>.
- [12] D. Brassard, M. Geissler, M. Descarreaux, D. Tremblay, J. Daoud, L. Clime, M. Mounier, D. Charlebois, T. Veres, Extraction of nucleic acids from blood: unveiling the potential of active pneumatic pumping in centrifugal microfluidics for integration and automation of sample preparation processes, *Lab Chip* 19 (11) (2019) 1941–1952, <https://doi.org/10.1039/c9lc00276f>.
- [13] K.J. Land, D.I. Boeras, X.S. Chen, A.R. Ramsay, R.W. Peeling, REASSURED diagnostics to inform disease control strategies, strengthen health systems and improve patient outcomes, *Nat Microbiol* 4 (1) (2019) 46–54, <https://doi.org/10.1038/s41564-018-0295-3>.
- [14] N.A. Khan, Z. Hasan, S.H. Jhung, Adsorptive removal of hazardous materials using metal-organic frameworks (MOFs): a review, *J. Hazard Mater.* 244–245 (2013) 444–456, <https://doi.org/10.1016/j.jhazmat.2012.11.011>.
- [15] A. Schaate, P. Roy, A. Godt, J. Lippke, F. Waltz, M. Wiebecke, P. Behrens, Modulated synthesis of Zr-based metal-organic frameworks: from nano to single crystals, *Chemistry* 17 (24) (2011) 6643–6651, <https://doi.org/10.1002/chem.201003211>.
- [16] L. Yu, Q. Xu, Y. Sun, Y. Wang, Y. Tang, Q. Yuan, S. Peng, G. Wu, Y. Xiao, X. Zhou, Programmable lanthanide metal-organic framework for ultra-efficient nucleic acids extraction and interaction analysis, *Anal. Chem.* 96 (28) (2024) 11455–11462, <https://doi.org/10.1021/acs.analchem.4c01839>.
- [17] S. Peng, B. Bie, Y. Sun, M. Liu, H. Cong, W. Zhou, Y. Xia, H. Tang, H. Deng, X. Zhou, Metal-organic frameworks for precise inclusion of single-stranded DNA and transfection in immune cells, *Nat. Commun.* 9 (1) (2018) 1293, <https://doi.org/10.1038/s41467-018-03650-w>.
- [18] Y. Sun, H. Yu, S. Han, R. Ran, Y. Yang, Y. Tang, Y. Wang, W. Zhang, H. Tang, B. Fu, B. Fu, X. Weng, S.M. Liu, H. Deng, S. Peng, X. Zhou, Method for the extraction of circulating nucleic acids based on MOF reveals cell-free RNA signatures in liver cancer, *Natl. Sci. Rev.* 11 (1) (2024) nwae022, <https://doi.org/10.1093/nsr/nwae022>.
- [19] W. Pan, X. Wang, X. Ma, Y. Chu, S. Pang, Y. Chen, X. Guan, B. Zou, Y. Wu, G. Zhou, Postsynthetic modification of the magnetic zirconium-organic framework for efficient and rapid solid-phase extraction of DNA, *ACS Appl. Mater. Interfaces* 13 (42) (2021) 50309–50318, <https://doi.org/10.1021/acsami.1c12622>.
- [20] Y.Y. Fu, C.X. Yang, X.P. Yan, Fabrication of ZIF-8@SiO₂ core-shell microspheres as the stationary phase for high-performance liquid chromatography, *Chemistry* 19 (40) (2013) 13484–13491, <https://doi.org/10.1002/chem.201301461>.
- [21] P. Sikorski, F. Mo, G. Skjak-Braek, B.T. Stokke, Evidence for egg-box-compatible interactions in calcium-alginate gels from fiber X-ray diffraction, *Biomacromolecules* 8 (7) (2007) 2098–2103, <https://doi.org/10.1021/bm0701503>.
- [22] S. Liu, H. Yang, D. Chen, Y. Xie, C. Tai, L. Wang, P. Wang, B. Wang, Three-dimensional bioprinting sodium alginate/gelatin scaffold combined with neural stem cells and oligodendrocytes markedly promoting nerve regeneration after spinal cord injury, *Regen Biomater* 9 (2022) rbac038, <https://doi.org/10.1093/rb/rbac038>.
- [23] S. Yang, L. Peng, O.A. Syzgantseva, O. Trukhina, I. Kochetygov, A. Justin, D.T. Sun, H. Abedini, M.A. Syzgantseva, E. Oveisi, G. Lu, W.L. Queen, Preparation of highly porous metal-organic framework beads for metal extraction from liquid streams, *J. Am. Chem. Soc.* 142 (31) (2020) 13415–13425, <https://doi.org/10.1021/jacs.0c02371>.
- [24] Z. Bai, Q. Liu, H. Zhang, J. Yu, R. Chen, J. Liu, D. Song, R. Li, J. Wang, Anti-biofouling and water-stable balanced charged metal organic framework-based polyelectrolyte hydrogels for extracting uranium from seawater, *ACS Appl. Mater. Interfaces* 12 (15) (2020) 18012–18022, <https://doi.org/10.1021/acsami.0c03007>.
- [25] K.C. Subbarao, G.S. Nattuthurai, S.K. Sundararajan, I. Sujith, J. Joseph, Y. P. Syedshah, Gingival crevicular fluid: an overview, *J. Pharm. BioAllied Sci.* 11 (Suppl 2) (2019) S135–S139, https://doi.org/10.4103/JPBS.JPBS_56_19.
- [26] K. Liu, B. Han, J. Hou, H. Meng, Preliminary investigation on the molecular mechanisms underlying the correlation between VDR-FokI genotype and periodontitis, *J. Periodontol.* 91 (3) (2020) 403–412, <https://doi.org/10.1002/JPER.19-0368>.
- [27] Y. Ma, Y. Chu, Z. Xu, C. Xie, X. Ma, L. Zhang, J. Hu, B. Zou, H. Wu, G. Zhou, Ultrafast and highly specific detection of one-base mutated cell-free DNA at a very low abundance, *Anal. Chem.* 96 (1) (2024) 117–126, <https://doi.org/10.1021/acs.analchem.3c03326>.